

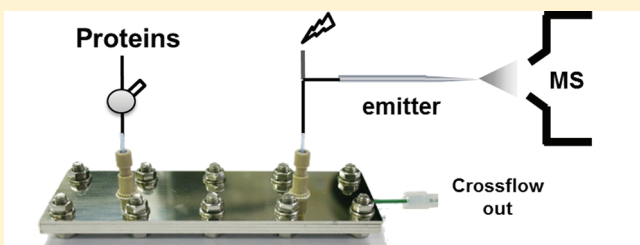
# Chip-Type Asymmetrical Flow Field-Flow Fractionation Channel Coupled with Mass Spectrometry for Top-Down Protein Identification

Ki Hun Kim and Myeong Hee Moon\*

Department of Chemistry, Yonsei University, 50 Yonsei-Ro, Seodaemun-Gu, Seoul 120-749, Korea

Supporting Information

**ABSTRACT:** A chip-type design asymmetrical flow field-flow fractionation (AF4) channel has been developed for high-speed separation of proteins and top-down proteomic analysis using online coupled electrospray ionization mass spectrometry (ESI-MS). The new miniaturized AF4 channel was assembled by stacking multilayer thin stainless steel (SS, 1.5 mm each) plates embedded with an SS frit in such a way that the total thickness of the channel assembly was about 6 mm. The efficiency of the miniaturized AF4 channel at different channel lengths was examined with the separation of protein standards by adjusting flow rates in which an identical effective channel flow rate or an identical void time can be maintained at different channels. Detection limit, overloading effect, reproducibility, and influence of channel membrane materials on separation efficiency were investigated. Desalting and purification of proteins achieved during the AF4 operation by the action of an exiting crossflow and the use of aqueous mass-spectrometry-compatible (MS-compatible) buffer were advantageous for online coupling of the chip-type AF4 with ESI-MS. The direct coupling of AF4 and ESI-MS capabilities was demonstrated for the high-speed separation and identification of carbonic anhydrase (29 kDa) and transferrin (78 kDa) by full scan MS and for the first top-down identification of proteins with AF4-ESI-MS-MS using collision-induced fragmentation (CID). The presence of intact dimers (156 kDa) of transferrin was confirmed by AF4-ESI-MS via size separation of the dimers from monomers, followed by multiply charged ion spectral analysis of the dimers and molecular mass determinations. It was also found from these experiments that AF4-ESI-MS analysis of transferrin exhibited an increased signal-to-noise ratio compared to that of direct ESI-MS analysis due to online purification of the protein sample and size separation of dimers with AF4.



Chip-type AF4 channel for Top-down Protein Identification

The field of proteomics has seen rapid growth due to the availability of modern ultrahigh-resolution mass spectrometry (MS), and a great number of proteomics applications are focused on life science problems. However, due to the complexity of proteome samples found in nature, high-performance separation of complex proteome samples is still a critical step regardless of whether a bottom-up or top-down proteomics approach is used. While bottom-up proteomics based on shotgun analysis of digested peptide mixtures provides excellent protein identification results,<sup>1–3</sup> this approach has some limitations in identifying peptides with modifications.<sup>4,5</sup> However, the top-down approach,<sup>6,7</sup> an alternate method for analyzing intact proteins (without enzymatic digestion) in the gas phase through various fragmentation processes, while challenging, offers direct analysis of the molecular masses of intact proteins and allows the identification of protein isoforms and posttranslational modifications (PTM).<sup>8–11</sup> Although top-down approach offers the above advantages, MS-compatible and highly efficient separation methods are still required to reduce sample complexity and to enhance protein identification in very complicated fragment ion spectra. Online intact protein separation has mostly been carried out with reverse-phase liquid chromatography (RPLC) using C4–C8 stationary phases in capillary columns,<sup>12,13</sup> reversed-phase non-porous silica columns,<sup>14</sup> or monolithic polymer columns.<sup>15</sup> Prior

to RPLC, weak anion exchange (WAX) chromatography<sup>9</sup> or gel-eluted liquid fraction entrapment electrophoresis (GELFrEE)<sup>12</sup> may have been utilized off-line to reduce the complexity of a protein mixture. RPLC in a capillary column provides robust separation of proteins in the nanoflow regime; however, the use of organic solvents may induce protein denaturation or dissociation of protein subunits, and the passage through packing materials may cause additional deformation or interaction of proteins with the stationary-phase surface.

Flow field-flow fractionation (flow FFF or F4), a variant of the FFF methods, is an elution technique for the separation of macromolecules or particulate species and has gained increasing interest as a size fractionation method for large biomolecules such as proteins, nanometer- to micrometer-sized subcellular species, cells, and natural aqueous polymers.<sup>16–18</sup> Separation by F4 takes place in an unobstructed channel space with a rectangular cross-section or in a hollow fiber (HF) membrane (HF-flow FFF or HF5) with a circular cross-section<sup>19,20</sup> and is achieved by the interaction of two independent flow streams, a migration flow moving along the channel axis and a crossflow

Received: August 11, 2011

Accepted: October 7, 2011

Published: October 08, 2011

(for rectangular channels) or radial flow (for HF) acting on the channel wall perpendicular to the channel axis. The size-sorting capability of F4 separation results from the differential migration of sample species depending on different diffusion rates (inversely proportional to the hydrodynamic size of the sample component) against the crossflow force acting on the channel wall, in which faster diffusing molecules (smaller size) travel further from the channel wall than do larger ones. Since the channel thickness is less than a few hundred micrometers, the migration flow generates a parabolic velocity distribution and results in the separation of molecules in increasing order of diameter. Since F4 separation is carried out in an open channel structure as well as in a biocompatible aqueous buffer solution, it is suitable for handling biomaterials in their intact states, with reduced concern for sample interaction with the separation system. Recent reports have demonstrated the potential of F4 in proteomics research as a powerful prefractionation method prior to mass spectrometry (MS) analysis. F4 has recently been utilized to fractionate bacterial cells,<sup>21</sup> mitochondria,<sup>22,23</sup> exosomes,<sup>24</sup> urinary proteome,<sup>25</sup> *C. Glutamicum* proteome,<sup>26</sup> and membrane proteins<sup>27</sup> in off-line combination with nanoflow liquid chromatography–electrospray ionization–tandem mass spectrometry (nLC-ESI-MS-MS). HF5 and F4 can be online coupled with isoelectric focusing (IEF) to develop gel-free two-dimensional separation devices, named CIEF-HF5 (C stands for capillary)<sup>28</sup> or IEF-AF4 (A prior to F4 stands for the asymmetrical design of F4 channel which has only one permeable wall),<sup>25,29</sup> respectively. In particular, IEF-AF4 provides high-speed 2D intact protein separation based on the differences in isoelectric point (pI) and hydrodynamic diameter ( $d_s$ ), and the resulting protein fractions from multilane AF4 channels are readily collected for further proteomic analysis. However, most of this work has been accomplished with off-line F4 separation, followed by bottom-up proteomic analysis in which the size-sorted proteins or subcellular species in each fraction need to be enzymatically cleaved for nLC-ESI-MS-MS, with the exception of an initial trial with online HF5-ESI-MS for the molecular mass determination of myoglobin (17.6 kDa) and hemoglobin.<sup>30</sup> The latter experiment demonstrated the possibility of directly coupling F4 with MS, but a significant splitting of the outflow (actual outflow rate of HF5 was 0.32 mL/min) was necessary. Further studies demonstrating top-down intact protein identification from fragment ion spectra generated by MS-MS analysis have not yet been carried out with the online F4-ESI-MS-MS configuration. One of the barriers to direct coupling of the F4 method with ESI-MS-MS is due to the technical difficulty of minimizing the outflow rate of the F4 system, which for typical protein separation conditions is approximately a few hundred microliters per minute. This problem could be overcome if the current F4 channels were miniaturized such that the outflow rate was reduced to a few microliters per minute scale, which could be directly fed into the ESI-MS without the need for significant splitting of the outflow.

Miniaturization of F4 has been attempted by reducing the geometrical dimensions of the asymmetrical F4 (AF4) channel<sup>22</sup> and by adopting microbore (i.d., 450  $\mu\text{m}$ ) hollow fibers<sup>31</sup> for HF5. The miniaturized AF4 channel was successfully operated at a minimum outflow rate of 50  $\mu\text{L}/\text{min}$  for protein separation. Microbore HF allowed the HF5 to be operated at a reduced outflow rate ( $\sim 10 \mu\text{L}/\text{min}$ ); however, it resulted in a substantial increase in retention time with band broadening unless the inner diameter of the HF was further reduced. The latter effect limits the loading capacity, which can result in a decreased sensitivity in

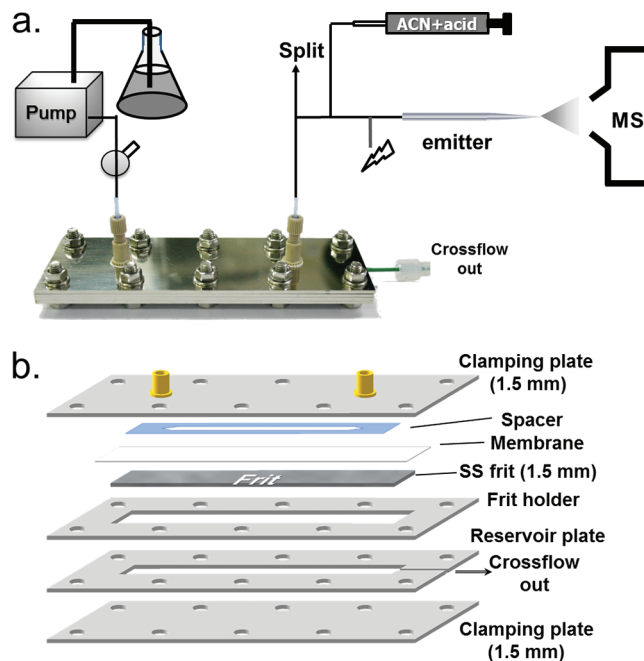


**Figure 1.** (a) Schematics of a chip-type miniaturized AF4 channel interfaced with electrospray ionization mass spectrometry (AF4-ESI-MS) and (b) the assembly of a chip-type AF4 channel.

top-down protein analysis coupled with MS. Moreover, a strong back-pressure in the fiber membrane is generated from the use of a capillary tip for ESI connected to the fiber end, which causes a fowling of fiber membrane.

In this study, a new chip-type channel design for miniaturized AF4 is introduced for high-throughput and high-speed separation of proteins with a very low rate of outflow, which is suitable for top-down protein identification from protein fragmentation with AF4-ESI-MS-MS. Since the new chip-type AF4 channel was assembled by stacking four 1.5-mm-thick stainless steel plates (see Figure 1), similar to other chip-type microscale separation devices, the channel itself was very thin ( $\sim 6 \mu\text{m}$ ) and was small enough to directly interface with the ESI-MS compared to that in typical AF4 channel blocks. To determine an efficient channel length of the miniaturized AF4, separation efficiency was first evaluated with protein standards by reducing the channel lengths (from 9 to 3 cm) under experimental conditions, producing an equivalent void time or an equivalent effective channel flow rate. Detection limit, overloading effect, reproducibility, and influence of channel membrane material on separation were investigated. The developed chip-type miniaturized AF4 channel with optimized channel dimensions was directly coupled to ESI-MS-MS as shown in Figure 1a and was tested for separation of protein standards and their dimers, followed by top-down protein identification from collision-induced dissociation. Since the miniaturized AF4 channel operates at a sufficiently low flow rate with a MS-compatible buffer and offers the simultaneous removal of salts and other impurities through the channel wall, it is more suitable for online coupling with ESI-MS to provide improved ionization efficiency compared with other chromatographic systems which require preliminary purification of sample materials. This study demonstrates the potential of chip-type AF4-ESI-MS-MS for the characterization of proteins from CID fragment ion spectra and also illustrates the capability of AF4-ESI-MS to

detect protein dimers through size fractionation by AF4 followed by MS analysis of multiply charged ions.

## EXPERIMENTAL SECTION

**Chip-Type Miniaturized AF4 Channel.** The chip-type miniaturized AF4 channel was constructed by stacking four layers of 1.5-mm-thick stainless steel (SS) plates as shown in Figure 1b. All of the SS plates with polished surfaces were cut with exterior dimensions of  $13 \times 4.5 \text{ cm}^2$  (Figure 1a). A sintered SS frit ( $10 \times 1.5 \times 0.15 \text{ cm}^3$ ) with an average pore size of  $5 \mu\text{m}$  was inserted into the frit holder SS plate (carved to fit the SS frit) and another SS layer to provide an inner space between the frit holder and the bottom plate as a flow reservoir underneath the frit, as shown in Figure 1b. The inner space for the reservoir was cut smaller ( $9.6 \times 1.1 \text{ cm}^2$ ) than the frit area such that the reservoir plate supported the frit. PEEK tubing (1/16 in. outer diameter) through which the crossflow will exit the reservoir was inserted into the conduit cut for the tubing exit and sealed with epoxy. Above the frit, a channel membrane and a spacer were layered in sequence. The channel space was cut from a poly(vinyl chloride) (PVC) sheet ( $254 \mu\text{m}$  in thickness) with a rectangular channel design (0.5 cm in width). To evaluate the effect of length on the miniaturized AF4, another conventional plastic channel design was utilized as described in the literature<sup>22</sup> by varying the tip-to-tip lengths to be 9, 7, 5, and 3 cm. Membrane materials were regenerated cellulose with a molecular mass cutoff (MMCO) of 20 kDa obtained from Millipore Corp. (Danvers, MA, USA), MWCOs of 5 and 10 kDa from Microdyn-Nadir GmbH (Wiesbaden, Germany), and polyethersulfone with a MWCO of 10 kDa from Microdyn-Nadir GmbH. The spacer, membrane, frit and frit holder, and reservoir plate were all clamped by two plain SS plates as shown in Figure 1b. The total thickness of the chip-type channel block was slightly more than 6 mm. On the upper plate, two holes were drilled (1/16 in. in diameter) for the flow inlet and outlet, and the tube connection was made through a Nanoport assembly from Upchurch Scientific (Oak Harbor, WA, USA), which was thermally fixed onto the SS surface. A Teflon tube was connected by insertion through the metal plate such that the tube end could be extended to the other surface of the upper SS plate.

**AF4-ESI-MS-MS.** The chip-type AF4 channel was evaluated by separation of protein standards, carbonic anhydrase from bovine erythrocyte (CA; 29 kDa), bovine serum albumin (BSA; 66 kDa), transferrin from bovine serum (78 kDa), and apoferritin from horse spleen (444 kDa) from Sigma (St. Louis, MO, USA). Carrier solution (10 mM  $\text{NH}_4\text{HCO}_3$  + 0.02%  $\text{NaN}_3$  in ultrapure water) was delivered to the AF4 channel with a model SP930D HPLC pump from Young-Lin (Seoul, Korea). Sample injection was accomplished with a model VI-12 loop injector with a 20  $\mu\text{L}$  loop from Flom (Tokyo, Japan), and the ratio of outflow/crossflow was adjusted by varying the length of a 50  $\mu\text{m}$  i.d. capillary tube for the outflow stream. Eluted protein species were monitored by a model M720 UV detector at 280 nm or by a LTQ Velos ion trap mass spectrometer from Thermo Finnigan (San Jose, CA, USA). AF4 outflow was introduced into the ESI-MS with a pulled tip capillary tube (17 cm  $\times$  100  $\mu\text{m}$  i.d., 360  $\mu\text{m}$  o.d.) as an emitter for ESI, as shown in Figure 1a. The AF4 outflow stream was first split to reduce the feeding flow rate (from 12 to 4  $\mu\text{L}/\text{min}$ ) using a micro-Tee from Upchurch Scientific and then mixed with ionization modifier liquid (1.0% formic acid in  $\text{CH}_3\text{CN}$  from a syringe pump) in a ratio of 1:4 (ionization modifier:AF4 out stream) via a NanoTight

Y connector with dual lumen sleeves from Upchurch Scientific. The final flow rate at the ESI-MS was 5  $\mu\text{L}/\text{min}$ . Ionization modifier was used to foster desolvation and protonation of proteins during ESI. ESI was carried out by applying electrical voltage through a Pt wire connected to a microcross (from Upchurch) at 2.0 kV, as shown in Figure 1a, and collision-induced dissociation (CID) for MS-MS experiments was achieved at  $m/z$  500–3000 of scan ranges for carbonic anhydrase and  $m/z$  500–4000 for transferrin and its dimer, 25–30% of the normalized collision energy, 10 ms of activation time, and 0.250 of  $q$ -value. Data were collected using Xcalibur software from Thermo Fisher Scientific. To calculate the intact masses of proteins, ProMass software from Novatia, LLC (Monmouth Junction, NJ, USA) was utilized to deconvolute the raw data. The  $m/z$  values of MS-MS fragments were compared with calculated  $m/z$  values of  $b$  and  $y$  fragment ions from amino acid sequences obtained from the Uniprot database (<http://www.uniprot.org/>). For this process, a list of  $m/z$  values of fragment ions with multiple charges was generated by using the software, Fragment Ion Calculator, and experimental data were compared with the list within the mass tolerance of 1.0 Da.

## RESULTS AND DISCUSSION

The miniaturized AF4 channel in this study was optimized by reducing the channel length to determine the minimum dimension that could separate proteins with a microflow rate regime suitable for direct feeding into the ESI-MS. The effect of AF4 channel length on protein separation was examined by decreasing the channel length from 9 to 7, 5, and 3 cm while maintaining a fixed width (0.5 cm). The three protein standards (carbonic anhydrase (29 kDa), BSA (66 kDa), and apoferritin (444 kDa)) were separated in the four different channels under experimental conditions providing an equivalent effective channel flow rate ( $\dot{V}_{\text{eff}}$ ) or an equivalent void time ( $t^0$ ). The void time of the AF4 channel can be expressed by the following equation:

$$t^0 = \frac{V^0}{\dot{V}_c} \ln \left( \frac{\dot{V}_{\text{out}} + \dot{V}_c}{\dot{V}_{\text{out}}} \right) = \frac{V^0}{\dot{V}_{\text{eff}}} \left( \dot{V}_{\text{eff}} = \dot{V}_c \left( \ln \left( \frac{\dot{V}_{\text{out}} + \dot{V}_c}{\dot{V}_{\text{out}}} \right) \right)^{-1} \right) \quad (1)$$

where  $V^0$  is the channel void volume and  $\dot{V}$  represents the volumetric flow rate at a location marked with each subscript: out for outflow and  $c$  for crossflow. To test the effect of channel length, the effective channel flow rate ( $\dot{V}_{\text{eff}}$ ) in eq 1 and field strength (or crossflow velocity at the channel wall,  $U = \dot{V}_c/bL$ , where  $b$  is for width and  $L$  for length) should be constant. Field strengths for the different channels could be adjusted by regulating  $\dot{V}_c$ , which was reduced according to the decrease in channel length. For each channel,  $\dot{V}_c$  was first determined, and then the outflow rate,  $\dot{V}_{\text{out}}$ , could be calculated to produce the same  $\dot{V}_{\text{eff}}$  for each channel (from the right side of eq 1). The ratio of equivalent channel flow velocity to crossflow velocity at the wall can be the same for all channels. Figure 2a shows the AF4 fractogram of protein separation with the four different channel lengths under identical ratios of effective channel flow velocity to crossflow velocity, in which the channel length effect could be visualized. The crossflow velocity used for the  $L = 9 \text{ cm}$  channel in the top fractogram of Figure 2a was 0.2 cm/min ( $0.85 \text{ cm}^3 \text{ min}^{-1}/(4.25 \text{ cm}^2)$ ). On the basis of the run conditions used in

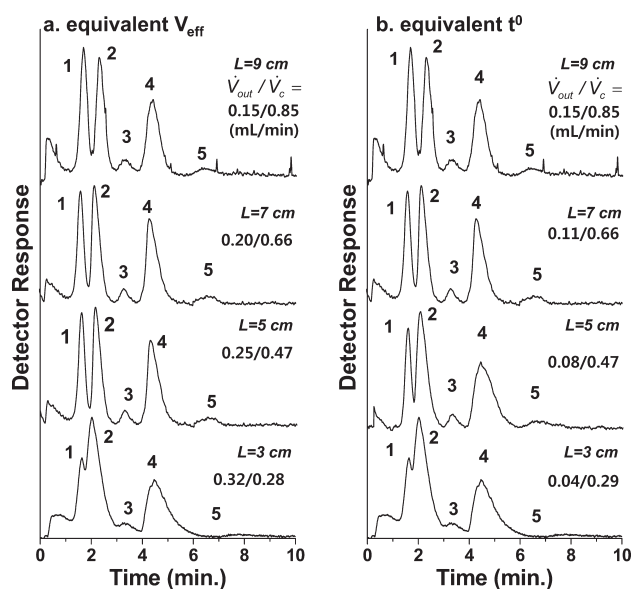


**Figure 2.** AF4 separation of protein standards (1, carbonic anhydrase (CA, 29 kDa); 2, bovine serum albumin (BSA, 66 kDa); 3, BSA dimer; 4, apoferritin (444 kDa); 5, apoferritin dimer) obtained with different channel lengths under run conditions producing (a) an equivalent effective channel flow rate ( $\dot{V}_{\text{eff}}$ ) and (b) equivalent void time ( $t^0$ ). Flow rate conditions are marked inside the figure.

the longest channel, the flow rate conditions needed for the other channel lengths were calculated and listed inside Figure 2a. The injection amounts for all of the runs in Figure 2 were  $0.5 \mu\text{g}$  of each protein standard, and the focusing/relaxation period was 2 min. For the AF4 channel with  $L = 9$  cm, proteins were separated as an increasing order of molecular mass along with dimers of BSA and apoferritin as peaks 3 and 5, respectively. As the channel length was decreased to 7, 5, and 3 cm, the eluted peaks became sharper, but the separation resolution deteriorated with the  $L = 3$  cm channel. The separation efficiency was the same for the first three channels on the basis of the measurement of plate height ( $H$ ) values of 0.48 mm ( $L = 9, 7,$  and  $5$  cm). The  $L = 3$  cm channel appeared to have a slightly better performance ( $H = 0.44$  mm), although the change was not significant. Similar experiments were carried out under run conditions that provided an equivalent void time, as shown in Figure 2b. The flow rate conditions marked in Figure 2b were calculated from eq 1 by selecting an outflow rate,  $\dot{V}_{\text{out}}$ , that produced the same  $t^0$  for all channels. To determine the run conditions for equivalent  $t^0$  with different channels,  $\dot{V}_{\text{eff}}$  needed to be adjusted for each channel according to the decrease in void volume with decreasing length. Once a field strength condition was determined for each channel, a new outflow rate condition could be calculated using eq 1. Since the void time and field strength condition were adjusted to be consistent for each channel, the retention time of each sample component should be the same for all of the channels with an equivalent void time. The apparent, relative variation in the retention time of apoferritin with the different channels was calculated to be 2%, which shows good reproducibility in the miniaturized AF4 operation. A resolution of separation ( $R_s$  for peaks 1 and 2) of  $0.95 \pm 0.14$  was achieved for the first three channels; however, it could not be measured with data from the  $L = 3$  cm channel due to significant peak overlap. Plate height values of apoferritin were measured to be 0.47, 0.45, 0.49, and

**Table 1.** Reproducibility of Retention Time and Experimental Plate Height of Protein Standards ( $n = 3$ )

protein	$t_r$ (min)	plate height (mm)
carbonic anhydrase	$1.76 \pm 0.00$	$0.86 \pm 0.09$
BSA	$2.57 \pm 0.00$	$0.57 \pm 0.05$
apoferritin	$5.51 \pm 0.05$	$0.37 \pm 0.03$

0.42 mm for the decreasing channel sizes. From the two sets of experiments, it was found that the length of the AF4 channel could be decreased to 5 cm without encountering a serious loss of separation efficiency. However, considering both convenience in flow control and separation resolution for small molecular mass proteins,  $L = 7$  cm was selected as an efficient length for the chip-type AF4 channel.

The throughput and detection limit of the chip-type AF4 channel ( $L = 7$  cm) were tested with BSA by varying the injection amounts (4, 2, 1, 0.5, 0.25, and  $0.10 \mu\text{g}$ ) under the run conditions ( $\dot{V}_{\text{out}}/\dot{V}_c = 0.20/0.66$  mL/min) listed in Figure 2a. An overloading effect was observed when the injection amount was greater than  $1 \mu\text{g}$ , and the limit of detection (LOD) was calculated to be 22.2 ng on the basis of an  $S/N = 3$  (signal-to-noise ratio) at a wavelength of 280 nm. The superimposed fractograms of BSA at different loading amounts were shown in Supporting Information Figure 1. Reproducibility of retention time and peak broadening was examined with the three protein mixture under run conditions of  $\dot{V}_{\text{out}}/\dot{V}_c = 0.15/0.71$  mL/min. The relative variations in retention time and plate height value of each component are listed in Table 1, which shows that less than 1% uncertainty in retention time and  $\sim 10\%$  variation in plate height were maintained.

The chip-type AF4 channel was tested with different membranes, shown in Supporting Information Figure 2, with the same protein standard mixtures under run conditions of  $\dot{V}_{\text{out}}/\dot{V}_c = 0.20/0.66$  mL/min. The membrane materials were RC (regenerated cellulose) with different pore sizes of (a) 20, (b) 10, (c) 5 kDa, and (d) PES (polyethersulfone) with 10 kDa. Since the RC membrane from Millipore had a relatively soft backing support, it was usually compressed when the channel plates were assembled. Compression of the membrane under the spacer resulted in a decrease in the actual channel thickness. However, with the stiffer RC membranes from Nadir, protein components eluted at longer retention times, as shown in fractograms b and c compared with fractogram a in Supporting Information Figure 2. The channel thickness,  $w$ , could be calculated from the measured retention times using FFF theory;<sup>16</sup> the calculated values were  $158.9 \mu\text{m}$  for the membrane used in run a and  $202.6 \mu\text{m}$  for runs b and c, while the geometrical spacer thickness was  $254 \mu\text{m}$ . It was notable that the signal intensity of peak 1 (CA, 29 kDa,  $0.5 \mu\text{g}$  injection for all) increased as the pore size of the RC membrane decreased to 5 or 10 kDa, indicating that some of the carbonic anhydrase was lost through the 20 kDa pore membrane. With the PES membrane, the retention time of peak 1 was further shifted to a longer time, implying that membrane compression was not significant and a greater effective channel thickness. For PES, the proper flow rate conditions needed to be adjusted to improve separation, but that work is not included in this report. From these experiments, Nadir 10 kDa RC was selected for continued evaluation in AF4-ESI-MS-MS. The maximum recovery of the chip-type AF4 channel was examined with BSA ( $0.5 \mu\text{g}$  injected) under the run conditions used in Supporting Information Figure 2 by

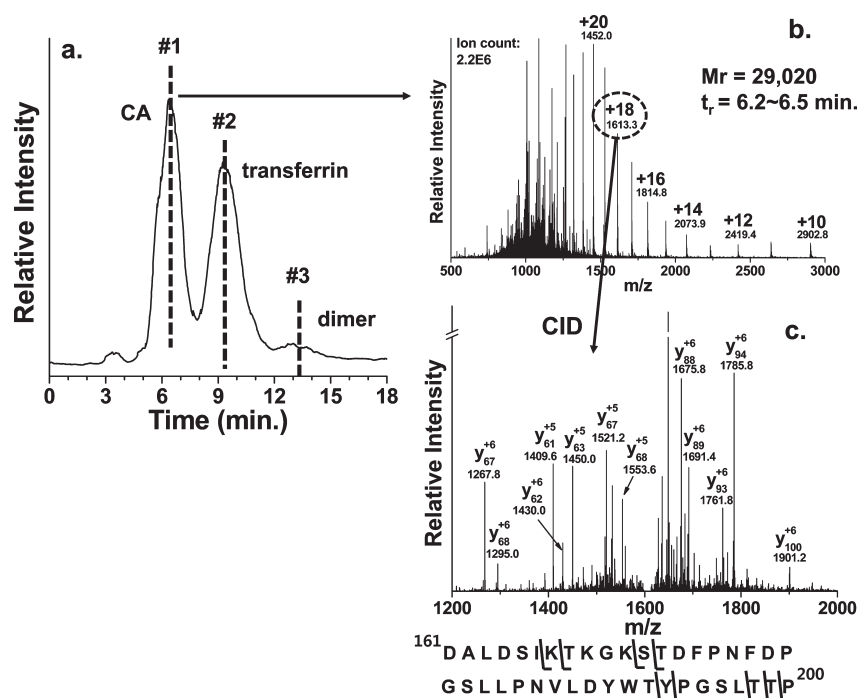


**Figure 3.** (a) Base peak fractogram (BPF) of AF4-ESI-MS for the separation of CA and transferrin obtained at  $\dot{V}_{\text{out}}/\dot{V}_c = 0.012/0.49$  mL/min, (b) full scan MS spectrum ( $m/z$  500–3000) of CA for no. 1 showing multiply charged ion peaks, and (c) CID spectrum ( $m/z$  1200–2000) of  $[M + 18H]^{+18}$  ( $m/z$  1613.3) along with the graphical fragmentation map of CA (161st–200th among 259 AA).

comparing the peak areas measured with and without an applied crossflow and was calculated to be  $74.7 \pm 6.52\%$  ( $n = 3$ ). This value was higher than reported recovery values of 57 to 47% at an outflow rate of 0.10 mL/min under crossflow rate conditions of 0.50–0.70 mL/min obtained from a similar AF4 channel (Lbw,  $9.3(0.7 \rightarrow 0.3$  cm, trapezoidal width)  $\times$   $0.0178$  cm<sup>2</sup>).<sup>22</sup>

Online coupling of AF4 with ESI-MS, configured as shown in Figure 1a, was tested with two protein standards to evaluate the capability for top-down protein identification from CID fragment ion spectra. Figure 3 shows (a) the base peak fractogram (BPF) of a separation of CA (29 kDa) and transferrin (78 kDa) from AF4-ESI-MS signals, along with (b) the AF4-ESI-MS of multiply charged CA molecules from the time slice of no. 1, and (c) CID spectra of  $[M + 18H]^{+18}$  ( $m/z$  1613.3) CA with characteristic  $y$ -series ions. The AF4 separation of CA (0.5  $\mu$ g) and transferrin (1.0  $\mu$ g) in Figure 3a was achieved under run conditions of  $\dot{V}_{\text{out}}/\dot{V}_c = 0.012/0.49$  mL/min. As shown in the diagram of AF4-ESI-MS in Figure 1a, outflow from the AF4 channel was split such that only one-third (4  $\mu$ L/min) of the volumetric flow rate was directed to the MS. The reduced outflow was merged with an ionization modifier liquid (1.0% formic acid in CH<sub>3</sub>CN) flow at 1  $\mu$ L/min from a syringe pump, resulting in a total flow rate of 5  $\mu$ L/min at the ESI-MS. AF4-ESI-MS was operated without extra sheath gas. The multiply charged ion spectra in Figure 3b yielded  $M_r$  of 29 020 Da using the deconvolution software, ProMass. Each MS spectrum was obtained from 100 microscans during elution (equivalent to a retention time interval of  $\sim 20$  s) as shown in the slice interval ( $t_r = 6.2$ – $6.5$  min) of no. 1 in Figure 3a. Figure 3c shows the CID spectra of  $[M + 18H]^{+18}$  ( $m/z$  1613.3) CA molecules representing multiply charged fragment ions with mostly  $y$ -series ions and the graphical fragmentation map of the transferrin amino acid sequence (from 161st to 200th of the total 259 amino acids).

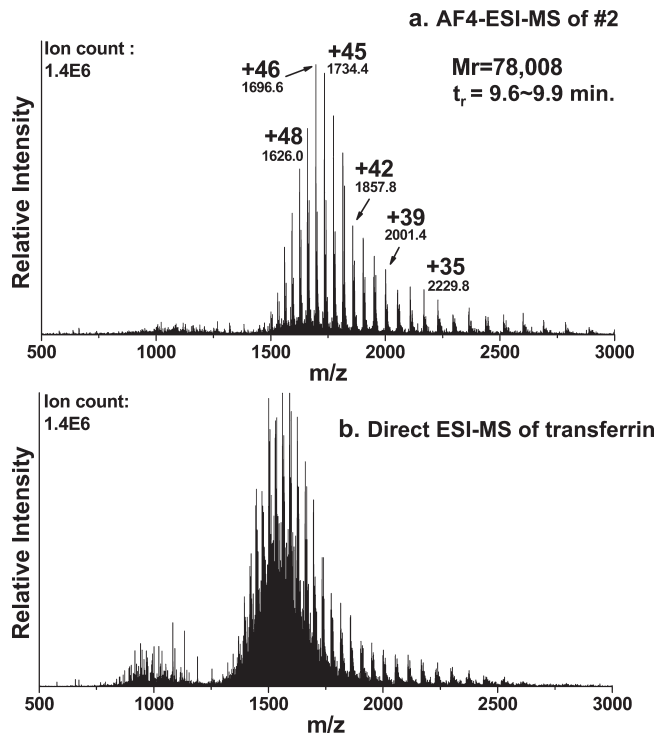


**Figure 4.** (a) Full scan AF4-ESI-MS for no. 2 (transferrin) shown in Figure 3a and (b) ESI-MS spectrum of transferrin (0.01  $\mu$ g/ $\mu$ L) by direct infusion at 5.0  $\mu$ L/min without AF4.

Similar results of AF4-ESI-MS-MS for transferrin (slice no. 2) are shown in Figure 4a for the MS scan of multiply charged ion spectra yielding a molecular mass of 78 008 Da along with

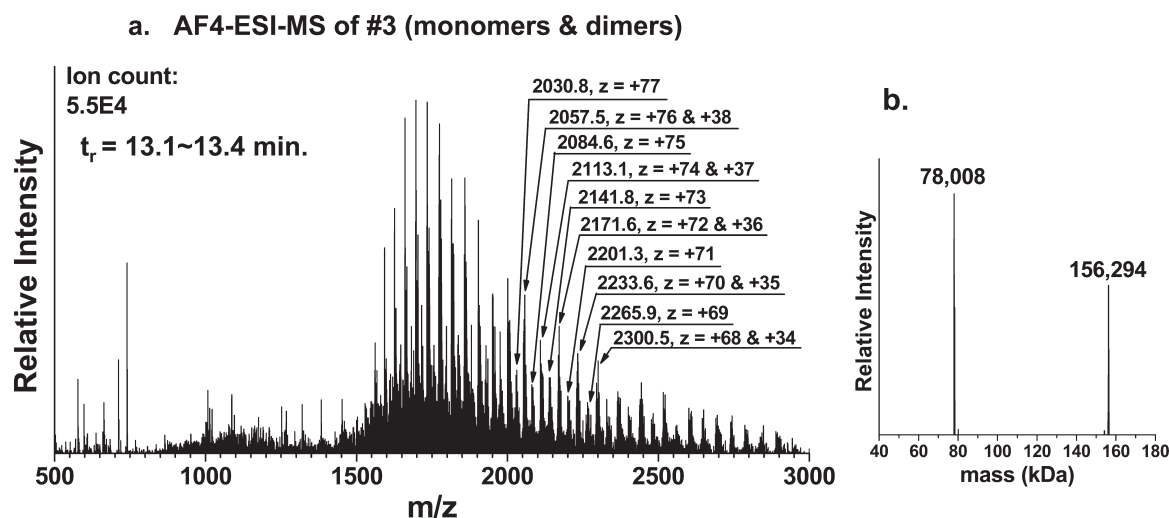


**Figure 5.** (a) AF4-ESI-MS spectrum of no. 3 (transferrin dimer) in Figure 3a showing mixed ion spectra of multiply charged monomers and dimers and (b) the deconvoluted MS spectrum showing transferrin monomer and dimer.

the data-dependent CID spectra of ions  $[M + 45H]^{+45}$  ( $m/z$  1734.4), which are shown in Supporting Information Figure 3. Supporting Information Figure 3 shows multiply charged fragment ions with mostly *b*-series ions and the graphical fragmentation map of the transferrin amino acid sequence (from 50th to 71st of the total 685 amino acids). In Figure 4b, a direct ESI-MS result of transferrin without using AF4 is shown for comparative purposes. Figure 4b was obtained by direct infusion of transferrin ( $0.01 \mu\text{g}/\mu\text{L}$  in 0.2% formic acid and 20%  $\text{CH}_3\text{CN}$ ) at the same feed flow rate of  $5.0 \mu\text{L}/\text{min}$ , which was adjusted to be the same as the feed flow rate in the AF4-ESI-MS experiment. To provide the same injection amount for ESI, maximum signal intensities of the two experiments were adjusted to be similar to each other ( $\sim 1.4 \text{ E}6$  for both) by controlling the protein concentration for the direct ESI-MS experiment.

The MS spectrum of multiply charged transferrin molecules in Figure 4a showed a relatively high *S/N* ratio compared to that obtained by direct infusion without AF4, shown in Figure 4b. The latter showed significant background noise, as well as a different distribution of multiply charged ions. The relatively low background noise in Figure 4a could be due to the ability of the AF4 to purify sample components online during the run and to resolve monomers from multimeric structures. Since proteins injected into the AF4 channel were subjected to a focusing/relaxation process prior to the separation, during which the two counterdirecting flow streams introduced from both the channel inlet and outlet were focused at a certain position ( $\sim 0.5 \text{ cm}$  from the inlet) of the channel to provide sample equilibrium, impurities or salts contained in the protein standard were washed through the channel membrane by the crossflow. Thus, online cleanup and desalting of proteins could be simultaneously achieved during the AF4 operation, and proteins could migrate in an intact state along the channel with the carrier solution containing MS-compatible salts. The ability to resolve protein aggregates can reduce spectral complexity, resulting in lower background noise in the multiply charged ion spectrum. This aspect of the method including evidence of the detection of transferrin dimers by AF4-ESI-MS will be discussed in the following section.

Figure 5a was obtained from the AF4 elution of no. 3 (marked in Figure 3a), which was presumed to be a dimer of transferrin.

Figure 5a was generated by merging 100 microscans to identify  $m/z$  values along with the charge state of transferrin dimer molecules in 13.1–13.4 min of retention time. Resolving dimer molecules from protein monomers by AF4 could be confirmed with a calibration curve, taking advantage of the relationship between retention time and molecular mass of protein standards, as described in an earlier report.<sup>22</sup>

However, identification of dimer molecules by ESI-MS cannot be easily established unless proper separation can be achieved, and only if dimer molecules remain intact without dissociation during ESI. The MS spectra in Figure 5a are clearly different from those in Figure 4a. Compared to the regularly distributed ion peaks of multiply charged transferrin monomers in Figure 4a, highly charged ion peaks of dimer molecules (i.e., +75 ions,  $m/z$  2084.6) were additionally found with a relatively weak intensity between two nearby ion peaks, of which each individual peak was expected to be caused by the overlap of two differently charged state ions, ( $z = +38$  for monomers and  $z = +76$  for dimers) and ( $z = +37$  for monomers and  $z = +74$  for dimers), respectively. However, the resolution of the current MS did not allow for distinction between the  $m/z$  values of the two different charge state ions. Deconvolution of the spectra in Figure 5a indicated the presence of the dimer peak at  $m/z$  156 294 Da, which is slightly larger than twice the molecular mass of the monomer (78 008 Da) observed, as shown in Figure 5b. Figure 5 provided support for the dissociation of some of the transferrin dimers into monomers during ESI and their detection together with the dimers. Since organic solvent stream with formic acid is merged with the FFF eluate prior to ESI (shown in Figure 1), a possible dissociation of dimer molecules can take place during the short transient period (less than 1 min). This experiment demonstrates that multimeric aggregates can be characterized utilizing AF4-ESI-MS at a high speed even with a sufficiently low flow rate.

## CONCLUSIONS

This study demonstrates the new assembly of a chip-type miniaturized AF4 system that can be directly coupled with ESI-MS-MS analysis for top-down protein identification. For effective online coupling, the channel outflow rate must be reduced to a few microliters per minute such that sample stream splitting is

not needed, while maintaining strong field strength conditions for both high-speed and high-efficiency separation. Especially for HF5 and AF4 channels, use of a high-speed radial flow or crossflow is conducive not only to the high resolution, but also to the speed of separation due to the simultaneous increase in  $\dot{V}_{\text{eff}}$  as shown in eq 1. However, due to the limitation in maximum radial flow rate for HF, miniaturization of the AF4 channel allows more flexibility for working at a very low outflow rate and at a high crossflow rate. The current work demonstrates for the first time AF4-ESI-MS-MS for protein separation at a low microflow rate regime along with CID experiments for the top-down identification of intact proteins up to 78 kDa and an observation of dimeric molecules of sizes up to 156 kDa from multiply charged ion spectra. By utilizing a sufficiently low outflow rate for AF4-ESI-MS, sample loss from splitting can be minimized, which is critical in dealing with low abundance proteins. Moreover, high-speed separation at such a low flow rate cannot be easily achieved with size exclusion chromatography or liquid chromatography even with the use of microcolumns. Another flexibility of AF4-ESI-MS is the direct injection of proteins or biological samples without preliminary desalting or exchange of solvent since impurities and other coexisting small molecules can be removed during the AF4 operation. Further studies are needed to expand the general applicability of the miniaturized AF4-ESI-MS-MS method for top-down protein identification of proteome samples using high-resolution MS.

## ■ ASSOCIATED CONTENT

**S Supporting Information.** Figures showing the overloading effect of a sample amount of BSA, effects of the membrane materials on the separation of protein mixtures, and the CID spectrum of  $[M + 45H]^{+45}$  ions. This material is available free of charge via the Internet at <http://pubs.acs.org>.

## ■ AUTHOR INFORMATION

### Corresponding Author

\*Phone: (82) 2 2123 5634. Fax: (82) 2 364 7050. E-mail: mhmoon@yonsei.ac.kr.

## ■ ACKNOWLEDGMENT

This study was supported by a grant (No.2010-0014046) from the National Research Foundation (NRF) of Korea funded by the Korean government (MEST).

## ■ REFERENCES

- (1) Henzel, W. J.; Billeci, T. M.; Stults, J. T.; Wong, S. C.; Grimley, C.; Watanabe, C. *Proc. Natl. Acad. Sci. U. S. A.* **1993**, *90*, 5011–5015.
- (2) Yates, J. R., III; Speicher, S.; Griffin, P. R.; Hunkapiller, T. *Anal. Biochem.* **1993**, *214*, 397–408.
- (3) Aebersold, R.; Mann, M. *Nature* **2003**, *422*, 198–207.
- (4) Cantin, G. T.; Yates, J. R., III *J. Chromatogr., A* **2004**, *1053*, 7–14.
- (5) Sharma, S.; Simpson, D. C.; Tolić, N.; Jaitly, N.; Mayampurath, A. M.; Smith, R. D.; Paša-Tolić, L. *J. Proteome Res.* **2007**, *6*, 602–610.
- (6) Loo, J. A.; Edmonds, C. G.; Smith, R. D. *Science* **1990**, *248*, 201–204.
- (7) Mørtz, E.; O'Connor, P. B.; Roepstorff, P.; Kelleher, N. L.; Wood, T. D.; McLafferty, F. W.; Mann, M. *Proc. Natl. Acad. Sci. U. S. A.* **1996**, *93*, 8264–8267.
- (8) Kelleher, N. L. *Anal. Chem.* **2004**, *76*, 196A–203A.

- (9) Parks, B. A.; Jiang, L.; Thomas, P. M.; Wenger, C. D.; Roth, M. J.; Boyne, I.; Burke, P. V.; Kwast, K. E.; Kelleher, N. L. *Anal. Chem.* **2007**, *79*, 7984–7991.
- (10) Armirotti, A.; Damonte, G. *Proteomics* **2010**, *10*, 3566–3576.
- (11) Thevis, M.; Ogorzalek Loo, R. R.; Loo, J. A. *J. Am. Soc. Mass Spectrom.* **2003**, *14*, 635–647.
- (12) Vellaichamy, A.; Tran, J. C.; Catherman, A. D.; Lee, J. E.; Kellie, J. F.; Sweet, S. M. M.; Zamdborg, L.; Thomas, P. M.; Ahlf, D. R.; Durbin, K. R.; Valaskovic, G. A.; Kelleher, N. L. *Anal. Chem.* **2010**, *82*, 1234–1244.
- (13) Chi, A.; Bai, D. L.; Geer, L. Y.; Shabanowitz, J.; Hunt, D. F. *Int. J. Mass Spectrom.* **2007**, *259*, 197–203.
- (14) Kachman, M. T.; Wang, H.; Schwartz, D. R.; Cho, K. R.; Lubman, D. M. *Anal. Chem.* **2002**, *74*, 1779–1791.
- (15) Mayr, B.; Hözl, G.; Eder, K.; Buchmeiser, M. R.; Huber, C. G. *Anal. Chem.* **2002**, *74*, 6080–6087.
- (16) Giddings, J. C. *Science* **1993**, *260*, 1456–1465.
- (17) Ratanathanawongs-Williams, S. K. In *Field-Flow Fractionation Handbook*; Schimpf, M. E., Caldwell, K. D., Giddings, J. C., Eds.; Wiley-Interscience: New York, 2000; pp 271–278.
- (18) Reschiglian, P.; Moon, M. H. *J. Proteomics* **2008**, *71*, 265–276.
- (19) Lee, W. J.; Min, B.-R.; Moon, M. H. *Anal. Chem.* **1999**, *71*, 3446–3452.
- (20) Reschiglian, P.; Zattoni, A.; Cinque, L.; Roda, B.; Dal Piaz, F.; Roda, A.; Moon, M. H.; Min, B. R. *Anal. Chem.* **2004**, *76*, 2103–2111.
- (21) Lee, H.; Williams, S. K. R.; Wahl, K. L.; Valentine, N. B. *Anal. Chem.* **2003**, *75*, 2746–2752.
- (22) Oh, S.; Kang, D.; Ahn, S. M.; Simpson, R. J.; Lee, B. H.; Moon, M. H. *J. Sep. Sci.* **2007**, *30*, 1082–1087.
- (23) Kang, D.; Oh, S.; Reschiglian, P.; Moon, M. H. *Analyst* **2008**, *133*, 505–515.
- (24) Kang, D.; Oh, S.; Ahn, S. M.; Lee, B. H.; Moon, M. H. *J. Proteome Res.* **2008**, *7*, 3475–3480.
- (25) Kim, K. H.; Moon, M. H. *J. Proteome Res.* **2009**, *8*, 4272–4278.
- (26) Kim, K. H.; Kang, D.; Koo, H. M.; Moon, M. H. *J. Proteomics* **2008**, *71*, 123–131.
- (27) Kang, D.; Yoo, J. S.; Kim, M. O.; Moon, M. H. *J. Proteome Res.* **2009**, *8*, 982–991.
- (28) Kang, D.; Moon, M. H. *Anal. Chem.* **2006**, *78*, 5789–5798.
- (29) Kim, K. H.; Moon, M. H. *Anal. Chem.* **2009**, *81* (4), 1715–1721.
- (30) Reschiglian, P.; Zattoni, A.; Roda, B.; Cinque, L.; Parisi, D.; Roda, A.; Dal Piaz, F.; Moon, M. H.; Min, B. R. *Anal. Chem.* **2005**, *77*, 47–56.
- (31) Kang, D.; Moon, M. H. *Anal. Chem.* **2005**, *77*, 4207–4212.